

Available online at www.sciencedirect.com

SCIENCE @ DIRECT®

Chemical Physics Letters 380 (2003) 34–41

**CHEMICAL
PHYSICS
LETTERS**www.elsevier.com/locate/cplett

A DFT study on the radical, monomer and dimer of α -keto pyruvic acid: equilibrium structures and vibrational analysis of stable conformers

X. Yang ^a, G. Orlova ^b, X.J. Zhou ^a, K.T. Leung ^{a,*}^a Department of Chemistry, University of Waterloo, Waterloo, Ont., Canada N2L 3G1^b Department of Chemistry, York University, Toronto, Ont., Canada M3J 1P3

Received 20 June 2003; in final form 31 August 2003

Abstract

The equilibrium structures and vibrational frequencies of the radical, monomer and dimer of α -keto pyruvic acid have been investigated by using hybrid density functional theory. The calculated geometries and the corresponding vibrational spectra of the three stable monomer conformers are found to be in good accord with earlier results. The present work provides the first detailed structure and vibrational analysis of the two stable dimer conformers, one of which is consistent with the X-ray diffraction and spectroscopic data, and also shows that there is only one stable form for the radical, with the others likely dissociated to the acetyl radical.

© 2003 Published by Elsevier B.V.

1. Introduction

The influence of molecular structure on the stability and reactivity of biomolecules has continued to be the focus of extensive recent studies, with the goal to develop better understanding for molecular design and control of the reaction pathways and biochemical outcomes [1–3]. As the main naturally occurring end-product of the metabolism of glucose in glycolysis in the body, α -keto pyruvic acid (CH_3COCOOH), or PA for short, has also attracted a considerable interest as an athletic performance enhancement and fat loss

drug [4,5]. Furthermore, the chelating sites provided by the carboxylic acid group and those by the keto group in PA offer structurally interesting bonding possibilities to other ligands or metal centres. Hydrogen bonding could also occur among the carboxylic acid group, the keto group and the methyl group. These bonding flexibilities generate different conformations in the PA monomer and dimer that are fundamentally interesting to biochemistry. Given that the methyl group is isoelectronic and similar in size to the hydroxyl component of the carboxylic acid group, PA could also be considered as a fairly ‘symmetric’ molecule.

The structural conformation and vibrational frequencies of PA have been investigated exten-

* Corresponding author. Fax: +1-519-7460435.

E-mail address: tong@uwaterloo.ca (K.T. Leung).

sively by various experimental [6,7] and theoretical [8–14] methods in the past 30 years. In particular, the conformation of PA monomers has been studied at the semi-empirical [8,11] and ab initio levels using Hartree–Fock (HF) [9,10] and MP2 methods [10,12], as well as density functional theory (DFT) [13,14]. Most of these theoretical studies have predicted the existence of four monomer conformers corresponding to different orientations of the O–H bond with respect to the C=O bond in the carboxylic acid group positioned in either the *trans* or *cis* configuration to the keto group [9,10]. An additional mirror set of four conformations can also be obtained by changing the orientation of the methyl group from the eclipsed to the staggered position [12,13]. Recently, Reva et al. [14] considered only the eclipsed conformers and predicted that three could exist naturally based on their experimental results and DFT calculation, which failed to converge on the least stable (the fourth) conformer. To the best of our knowledge, a comprehensive computational study of all possible conformers for the monomer has not been reported. In the present work, the stability and geometry of the monomer conformers have been determined using the hybrid DFT method. Of the ‘converged’ conformations (four eclipsed and three staggered forms) obtained in the present work, further vibrational analysis shows that only three eclipsed conformers exist, confirming the results of Reva et al. [14]. In addition, X-ray diffraction data and vibrational spectra revealed that PA in the solid phase could form a dimer structure via hydrogen bonding and further suggested the presence of only one possible dimer structure [15,16]. To date, no other experimental or theoretical study has been performed to fully explore the existence of other stable dimer structures due to the number of possible conformers of the PA monomer. After comparing the present calculation with the experimental data [15,16], we isolate two stable conformers for the dimer. As a prelude to future adsorption studies on metal surfaces [17], we also investigate the radical of PA in order to gain some insight into the possible bonding structure and reaction pathways. The present calculation is therefore of interest to metal surface chemistry because radical formation of an

organic acid (via dehydrogenation of the hydroxyl group) is quite common upon adsorption on (transition) metal surfaces [18,19].

2. Computational details

The total electronic energies, equilibrium geometries and corresponding harmonic vibrational frequencies of possible conformations of the radical, monomer, and dimer of PA have been determined by using the hybrid DFT method at the B3LYP (Becke’s three-parameter hybrid functional using the Lee–Yang–Parr correlation functional) level [20,21]. Geometry pre-optimization and vibrational analysis were carried out by using the 6-31G basis set and the final geometries were fully optimized by using the larger 6-311++G(3df, 3pd) basis set, which has been found to be capable of giving more reliable hydrogen-bonding interaction energies [22]. All the calculations have been performed using the GAUSSIAN 98 suite of programs [23] at a home-built technical compute farm based on the Pentium-4 technology. Calculations for the total energies and relative stabilities as well as the binding energies reported in the present work have included the zero-point vibrational energy (ZPVE) corrections. The atom labelling and other nomenclature of the PA monomer used in the present work follow that of [10,13]. In particular, the dihedral angle $C_{\text{methyl}}-C_{\text{keto}}-C_{\text{acid}}-O_{\text{hydroxyl}}$ of 0° and 180° is labelled by an upper-case letter C (for *cis* form) and T (for *trans* form), respectively, while the dihedral angle $C_{\text{keto}}-C_{\text{acid}}-O-H$ of 0° and 180° is labelled by a lower-case letter c (for *cis* form) and t (for *trans* form), respectively. The eclipsed and staggered orientation of the methyl group with respect to the keto group, with the corresponding dihedral angle $H_{\text{methyl}}-C_{\text{methyl}}-C_{\text{keto}}=O_{\text{keto}}$ of 0° and 180° , is denoted by a lower-case letter e and s, respectively. In the case of the dimer, we append the letter D to the associated monomer label to indicate its conformation. To facilitate better comparison with the experimental data [7,16], the calculated vibrational frequencies above 1100 cm^{-1} obtained in the present work have been reduced semi-empirically by 2% (as has been done in the earlier studies [24,25]).

3. Results and discussion

3.1. Equilibrium structures, total energies and dipole moments of conformers

Table 1 shows the equilibrium structures and the corresponding total energies and dipole moments for the stable conformers of the radical, monomer

and dimer of PA. In the case of the monomer and dimer, the optimized geometries are also compared with the available experimental data reported in the literature [6,15]. All the staggered structures are found to have not only a higher total energy than the corresponding eclipsed forms but also imaginary vibrational frequencies. The presence of imaginary frequencies generally indicates that the

Table 1

Optimized geometries, total energies and relative stabilities, and dipole moments for the radical and stable conformers of the monomer and dimer of α -keto pyruvic acid

	Radical	Monomer					Dimer			
		Tce	Tte	Cte	Cce	Exp [6]	Tte-D	Cte-D	Exp [15]	
Bond lengths (Å)										
C2–C1	1.494	1.492	1.501	1.503	1.513	1.486	1.501	1.502	1.487	
C3–C2	1.540	1.552	1.551	1.558	1.567	1.523	1.554	1.558	1.529	
O4–C2	1.201	1.209	1.201	1.199	1.197	1.231	1.200	1.199	1.206	
H5–C1	1.092	1.091	1.091	1.091	1.093	1.106	1.091	1.091	1.200	
H6–C1	1.086	1.086	1.086	1.086	1.086	1.074	1.086	1.086	0.930	
H7–C1	1.092	1.091	1.091	1.091	1.093	1.106	1.091	1.091	1.120	
O8–C3	1.239	1.332	1.336	1.351	1.354	1.328	1.303	1.313	1.311	
O9–C3	1.259	1.198	1.203	1.194	1.189	1.215	1.222	1.215	1.218	
H10–O8		0.974	0.969	0.969	0.963	0.983	0.999	1.003	1.190	
O19–H10							1.670	1.649		
Bonds angles (°)										
C3–C2–C1	117.0	117.0	114.7	117.9	118.8	118.6	115.3	117.4	116.0	
O4–C2–C1	126.3	125.3	124.9	124.3	123.0	124.4	124.9	124.5	123.8	
H5–C1–C2	109.7	109.6	110.0	110.2	110.9	109.0	110.2	110.2		
H6–C1–C2	110.3	110.1	109.5	109.4	109.2	110.7	109.4	109.3		
H7–C1–C2	109.7	109.6	110.0	110.2	110.9	109.0	110.2	110.2		
O8–C3–C2	124.8	112.7	112.6	111.7	116.5	114.5	113.9	113.2	114.5	
O9–C3–C2	120.7	123.1	122.8	124.2	122.2	122.0	120.4	121.3	121.2	
H10–O8–C3		107.1	107.5	107.5	111.9	105.2	110.6	110.8		
O19–H10–O8							178.8	178.1		
Dihedral angles (°)										
O4–C2–C1–C3	180.0	180.0	180.0	180.0	180.0		180.0	180.0		
H5–C1–C2–O4	–121.7	122.0	121.7	121.4	120.0		121.6	121.5		
H6–C1–C2–O4	0.0	0.0	0.0	0.0	0.0		0.0	0.0		
H7–C1–C2–O4	121.7	–122.0	–121.7	–121.4	–120.0		–121.6	–121.5		
O8–C3–C2–C1	0.0	180.0	180.0	0.0	0.0		180.0	0.0		
O9–C3–C2–C1	180.0	0.0	0.0	180.0	180.0		0.0	180.0		
H10–O8–C3–C2		0.0	180.0	180.0	0.0		180.0	180.0		
O19–H10–O8–C3							0.0	0.0		
Total energy (hartree)	–341.795822	–342.468619						–684.950414		
Relative stability ^a (kJ/mol)		0 (3.05)	10.74 (14.30)	17.21 (22.26)	43.35		0	5.0		
Dipole moment ^a (Debye)	3.43	2.38 (2.47)	1.27 (1.17)	4.06 (3.97)	5.51		0.0	0.0		

^a The values shown in parentheses correspond to the staggered conformers.

staggered structures do not correspond to local minima on the respective potential energy hypersurfaces. The staggered structures are therefore not considered further in the present work. Fig. 1 shows the equilibrium structures of the stable conformers of the radical, monomer and dimer in the eclipsed form. Evidently, the C–C bond lengths in the optimized geometries are slightly larger than the corresponding experimental ones for both the monomer and dimer conformers (Table 1). In particular, the standard deviations of the calculated bond lengths from the experimental ones for the Tce and Tte monomer conformers are found to be 1.6% and 1.8%, respectively, while those for the Cte (2.2%) and Cce conformers (2.6%) are slightly higher. The magnitudes of the observed derivations in the bond lengths are consistent with the ordering of the calculated energies of the conformers, with the Tce conformer being the most stable monomer with total energy of -342.468619 hartrees. With the total energies only slightly higher than that of Tce by 10–18 kJ/mol, the existence of Tte and Cte conformers could also be viable. The present calculation is in good agreement with all the earlier studies [8–10,12–14], which affirms the validity of the present computational method. In contrast to the more involved HF and MP2 calculations by Reva et al. [14] that did not show convergence for the least stable Cce conformer, the present DFT calculation shows that the corresponding total energy converged at 43.35 kJ/mol above the Tce minimum. Using the same basis set (aug-cc-pVDZ) as that employed by Reva et al. [14], we repeated the DFT calculation and found identical energies and relative stabilities as those obtained by Reva et al. for the other three stable eclipsed conformers. In the case of the Cce conformer, the calculated total energy is however found to converge at 48.85 kJ/mol above the Tce minimum. Further vibrational analyses using both basis sets reveal the existence of an imaginary frequency, which suggests that the Cce conformer is not a true minimum on the potential energy hypersurface. We therefore conclude that only three of the eclipsed structures (Tce, Tte, and Cte) for the PA monomer calculated in the present work correspond to true local minima on the potential energy surface for both 6-311++G(3df, 3pd) and aug-cc-pVDZ basis sets.

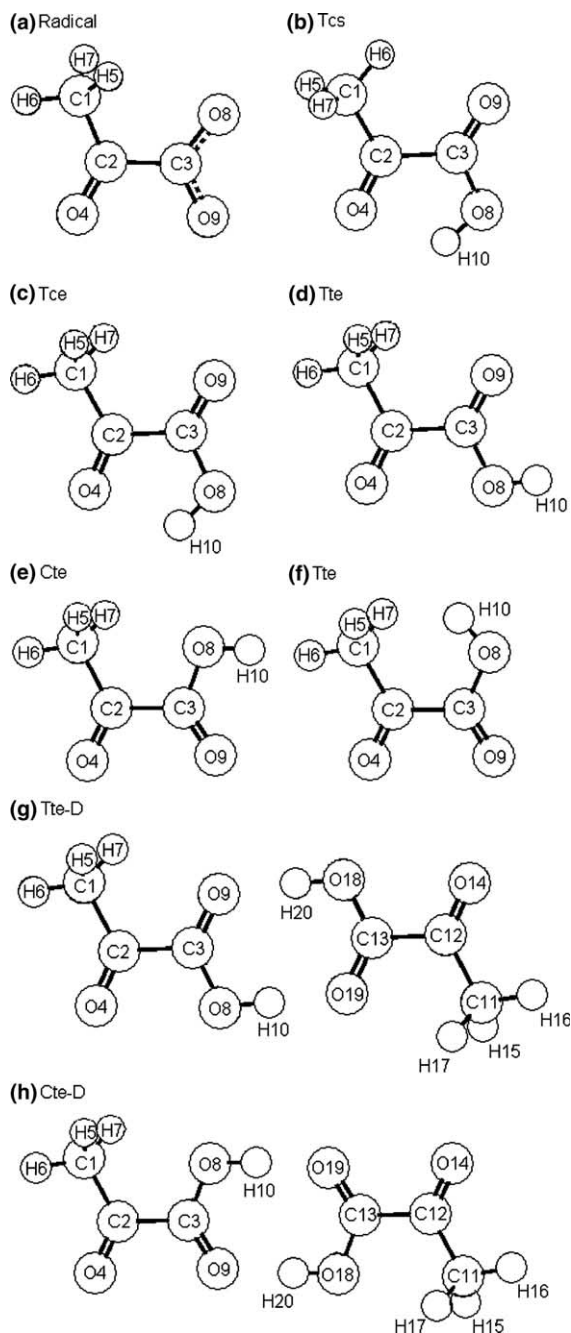


Fig. 1. Calculated equilibrium structures of the conformers for the radical, monomer and dimer of α -keto pyruvic acid.

The two stable conformers for the dimer shown in Fig. 1g,h are obtained by linking two monomers together by hydrogen bonding between the

carboxylic acid groups with an approximate bond length (O9-H20 or H10-O19) of 1.66 Å. Both dimer conformers (with C_{2h} symmetry) are found to have a planar backbone structure with an inversion centre. Because both the optimized geometries and experimental structures show that the geometries of individual monomers in the dimer are identical to each other, we only give the structural parameters for one of the (identical) monomers in Table 1. The bond lengths, dihedral angles and most other bond angles of a monomer in both dimer conformers are found to be similar to the corresponding values of a stand-alone monomer. The only exception is that the bond angle of H10-O8-C3 (and H20-O18-C13) of the dimer (Fig. 1g) is slightly larger than that of the monomer by 3–4°, while the bond angle of O9-C3-C2 (and O19-C13-C12) of the dimer is smaller than that of the monomer by 2–3°. These discernible differences are due to the effect of hydrogen bonding between the H and O atoms in different monomers. Furthermore, the total energy of the more stable Tte-D conformer (at –684.950414 hartrees) is found to be only slightly lower than the Cte-D conformer by 5.0 kJ/mol (Table 1). The small energy difference suggests that both dimer conformers could exist in the solid phase. The standard deviations of optimized structural parameters for both the Tte-D (9.1%) and Cte-D (9.0%) conformers (from the corresponding experimental ones) are similar and also consistent with the similar values of the calculated total energies, which further supports the hypothesis that both structures could exist naturally. The calculation also shows a large binding-energy value (counterpoise-corrected) for both stable PA dimers with –54.03 and –62.02 kJ/mol for the Tte-D and Cte-D conformers, respectively. The function counterpoise corrections for the basis set superposition error (BSSE) [22,26] for both dimers are quite similar (2.04 kJ/mol for Tte-D and 1.95 kJ/mol for Cte-D). The present binding energy results for the PA dimers are found to have similar values as the dimers of related organic acids (formic acid, acetic acid, propionic acid, butyric acid and isobutyric acid) obtained by using the same method as reported by Hintze et al. [27].

Removal of the hydrogen from the hydroxyl group produces an interesting radical structure

with two sets of possible chelating C=O groups separated by 2.722 Å (between the keto group and carboxyl radical group) and 2.101 Å (within the carboxyl radical group). The relative eclipsed orientations of the carboxyl radical group with respect to the keto group (with dihedral angles of 0°, 90° and 180°) in the α -keto PA radical ($\text{CH}_3\text{CO}\cdot\text{COO}\cdot$) would generate three possible conformations, which have also been determined by DFT calculations at the unrestricted B3LYP/6-311++G(3df,3pd) level in the present work. Both non-planar eclipsed radical structures are found to decompose into CO_2 and $\text{CH}_3\text{CO}\cdot$ (the acetyl radical), while the planar eclipsed radical structure (with C_s symmetry) is found to converge after several cycles of optimization (Fig. 1a). The present result indicates only one stable structure for the PA radical, the optimized structural parameters of which are found to be similar to those of the PA monomer conformers (Fig. 1c–e), with the corresponding standard derivations of 4.0% for Tce and Tte and 4.6% for Cte monomer conformers (Table 1). Furthermore, the total energy of the PA radical (–341.795822 hartrees, Table 1) is found to be 138.04 kJ/mol higher than the sum of the total energies of the dissociated products (CO_2 and $\text{CH}_3\text{CO}\cdot$), which indicates that the PA radical is not thermodynamically stable. However, the calculation shows a small but discernible dissociation barrier (11.5 kJ/mol), which suggests that the formation of the PA radical on a surface could be viable due to the stabilization effects from the (transition) metal substrate atoms [18].

3.2. Vibrational analysis

Along with their relative intensities, the vibrational frequencies of the PA radical, monomer and dimer obtained by the present DFT calculation are compared with the corresponding experimental data [7,16] in Table 2. The calculated frequencies for the stretching vibrations for both the monomer and dimer appear to have larger variations from the corresponding experimental frequencies than those of the other vibrational modes. Similar variation has also been reported for the vibrational frequencies of the Tce conformer obtained in an

Table 2

Comparison of the calculated vibrational frequencies (cm^{-1}) and corresponding intensities (in the parentheses) of the radical, the monomer and dimer conformers of α -keto pyruvic acid with the corresponding experimental data

Vibrational mode ^a	Radical	Monomer				Dimer ^b		
		Tce	Tte	Cte	Exp [7]	Tte-D	Cte-D	Exp [16]
$\nu(\text{OH})$		3564 (32)	3674 (30)	3665 (28)	3432	3127 (100)	3074 (100)	3100
$\nu_{\text{as}}(\text{CH}_3)$	3089 (3)	3094 (1)	3093 (2)	3087 (3)	3033	3093 (2)	3091 (2)	3025
$\nu_{\text{as}}(\text{CH}_2)$			3037 (1)	3036 (1)				2942
$\nu_s(\text{CH}_3)$	2973 (3)				2936			
$\nu(\text{C}2=\text{O}4)$, $\delta(\text{CCC})$	1778 (82)	1807 (74)	1778 (68)	1782 (100)	1800	1781 (8)	1784 (6)	1771
$\nu_{\text{as}}(\text{COO})$, $\delta(\text{COH})$	1517 (30)	1749 (32)	1765 (100)	1803 (64)	1729	1720 (18)	1747 (18)	1728
$\delta_{\text{as}}(\text{CH}_3)$	1431 (9)	1430 (3)	1433 (4)	1439 (4)	1425	1434 (1)	1438 (1)	1452
$\delta_{\text{as}}(\text{CH}_3)$, $\delta(\text{COH})$	1423 (10)	1427 (4)	1430 (6)	1433 (10)	1424		1438 (2)	1426
$\delta_s(\text{CH}_3)$, $\nu_{\text{as}}(\text{CCC})$, $\delta(\text{COH})$	1366 (31)	1374 (2)	1370 (4)	1368 (16)	1384	1367 (2)	1367 (2)	1361
$\delta_s(\text{CH}_3)$, $\delta(\text{COH})$, $\nu(\text{C}1\text{C}2)$		1349 (100)						
$\delta(\text{COH})$, $\nu_{\text{as}}(\text{C}2\text{C}3\text{O}8)$			1347 (16)	1310 (6)		1304 (5)	1282 (8)	1273
$\delta(\text{COH})$, $\nu_{\text{as}}(\text{CCC})$, $\gamma(\text{CH}_3)^c$	1178 (77)	1218 (24)	1194 (12)	1162 (42)	1214	1151 (8)	1152 (7)	1166
$\gamma(\text{CH}_3)$, $\delta(\text{COH})$, $\nu_{\text{as}}(\text{CCC})$		1133 (19)	1118 (92)	1109 (96)	1137	1440 (2)		
$\nu_{\text{as}}(\text{COO})$, $\delta(\text{CCC})$	1103 (100)							
$\gamma(\text{CH}_3)$, $\tau(\text{CCC})$	1040 (1)		1042 (1)	1045 (1)		1046 (1)	1052 (2)	1057
$\gamma(\text{CH}_3)$, $\nu_{\text{as}}(\text{CCC})$, $\delta(\text{COH})^c$	961 (36)	981 (6)	971 (18)	978 (10)	969	978 (1)	982 (1)	983
$\nu_s(\text{CCC})$, $\delta(\text{COO})$	747 (1)	766 (2)	739 (5)	730 (5)	762	804 (1)	800 (1)	
$\gamma(\text{CH}_3)$, $\tau(\text{CCC})$, $\tau(\text{COH})^d$	686 (6)	742 (5)	736 (17)	735 (20)	720			
$\gamma(\text{CH}_3)$, $\tau(\text{COH})$, $\tau(\text{CCC})$		704 (23)	624 (35)	618 (34)	664	1022 (4)	1031 (3)	1027
$\delta(\text{OCCO})$	599 (20)	610 (5)	597 (30)	612 (15)	604	623 (2)	625 (3)	626
$\delta(\text{CCC})$, $\delta(\text{CCCCO}8)^e$		525 (1)	514 (1)	481 (3)	535	538 (2)	527 (1)	553
$\tau(\text{OCCO})$, $\tau(\text{CCC})$	375 (15)	399 (5)						
$\delta(\text{CCC})$, $\delta(\text{OCCO})$	353 (1)	391 (3)		399 (1)	388	312 (3)		
$\delta(\text{CCC})$	183 (8)	253 (7)	249 (4)	256 (1)	258			225
ω							96 (1)	
$\tau(\text{OCCO})$, $\tau(\text{COO})$, $\gamma(\text{CH}_3)$	63 (2)	90 (2)	32 (3)		90			

^a Legends: ν_s = symmetric stretching mode; ν_{as} = asymmetric stretching mode; δ = bending mode; γ = rocking mode; τ = torsion mode; ω = wagging mode of the adjoining monomers.

^b The corresponding IR inactive vibrational frequencies (from top to bottom) for the Tte-D conformer are 3022, 3093, 1781, 1659, 1434, 1367, 1299, 1154, 1468, 1044, 977, 779, 986, 616, 526 and 312 cm^{-1} , while those for the Cte-D conformer are 2963, 3090, 1784, 1691, 1438, 1429, 1367, 1269, 1156, 1046, 982, 777, 1001, 624, 504 and 125 cm^{-1} .

^c The vibrational features only occur in the Cte conformer.

^d The vibrational feature only occurs in the Tce conformer.

^e For the Cte and Cte-D conformers, the corresponding vibrational feature is $\delta(\text{CCCCO}9)$.

earlier calculation by Zhou et al. [13]. These observations can be explained by the systematic errors in the basis sets and/or by the lack of anharmonicity included in the calculations, the latter of which becomes more evident in the case of stretching modes [13].

Evidently, the discernible presence of the $\nu_{\text{as}}(\text{CH}_2)$ bending mode near 3036 cm^{-1} , the $\gamma(\text{CH}_3)$ rocking mode near 735 cm^{-1} and the $\delta(\text{CCC})$ bending mode near 250 cm^{-1} in the PA monomer conformers but not in the dimer conformers is due to the inversion symmetry of the dimer. It is also of interest to note that a weak monomer wagging mode at 96 cm^{-1} is found in the Cte-D dimer. Among all other vibrational features, the $\nu(\text{OH})$ stretching mode is found to be at a discernibly lower frequency in the dimer ($\sim 3100\text{ cm}^{-1}$) than the corresponding monomer ($\sim 3670\text{ cm}^{-1}$), which could be attributed to the hydrogen bonding in the dimer. The calculated frequencies of both stable conformers for the dimer are similar to each other and are in good accord with the experiment [16], which further supports our hypothesis that both conformers may coexist. Furthermore, it is of interest to note that in accord with the zero overall dipole moment for the dimer conformers (Table 1), most of their vibrations are found to be weak except for the $\nu(\text{OH})$ stretching mode. This is in marked contrast to the corresponding Tte and Cte monomer conformers, in which the $\nu_{\text{as}}(\text{COO})$ stretching mode at 1765 cm^{-1} and $\nu(\text{C}=\text{O})$ stretching mode at 1782 cm^{-1} , respectively, are found to be the strongest.

With the absence of the OH group in the PA radical, the $\nu_{\text{as}}(\text{COO})$ anti-symmetric stretching mode of the carboxyl radical group at 1103 cm^{-1} becomes the strongest vibrational feature, in contrast to the OH related vibrations in the case of the monomer and dimer conformers. The frequencies of the other vibrational modes in the radical are found to be similar to those of the monomers, especially for the Tte conformer in which the OH group is expected to have the least influence on the other functional groups. The vibrations involving the COO and CCC groups in the radical are therefore more prominent than those in the monomer conformers, in which the vibrations involving the OH and CH_3 groups dominate.

4. Concluding remarks

We have carried out DFT calculations at the B3LYP level with a 6-311++G(3df, 3pd) basis set to determine the equilibrium structures and vibrational frequencies of the stable conformers for the radical, monomer and dimer of α -keto pyruvic acid. Three stable conformations in the eclipsed form for the monomer have been identified and their corresponding structures and vibrational frequencies are found to be in good accord with the earlier calculations [8–14] and experimental data [6,7,14]. Using the same method, we have provided the first detailed evaluation of the stable structures for the PA radical and for the two stable dimer conformers. In the case of the dimer, the calculated vibrational frequencies are also found to be in good agreement with an earlier experimental study [16]. The structures of the PA radical, monomer and dimer conformers obtained in the present work are of the eclipsed rather than staggered form. The present calculation also suggests that both dimer conformations are plausible and the similarities of their calculated vibrational spectra make differentiation of individual dimer conformers difficult. In the case of the radical, the present calculation shows that except for the reported stable structure (Fig. 1a) the other radical conformers would undergo dissociation into CO_2 and $\text{CH}_3\text{CO}\cdot$. The calculation also shows that even though the radical is not thermodynamically stable, it could be stable on the surface due to the presence of a dissociation barrier and possible stabilization effects. In a follow-up study [17], we will extend the present DFT calculations to investigate the interactions of PA with Ni atoms and model Ni clusters and to compare them with our surface vibrational data obtained on Ni(100) under ultrahigh vacuum conditions. In combination with the present calculations, our experiment gives clear evidence for the presence of the PA radical, which could be readily formed by dehydrogenation upon adsorption on Ni(100) at room temperature.

Acknowledgements

It is our pleasure to acknowledge Professor John Goddard (University of Guelph) and Mr.

Sergey Mitlin for helpful discussion. This work was supported by the Natural Sciences and Engineering Research Council of Canada.

References

- [1] H. Tsujishita, S. Hirono, *J. Comput.-Aided Mol. Des.* 11 (1997) 305.
- [2] M.D. Paulsen, J.R. Rustad, B.P. Hay, *J. Mol. Struct. (Theochem.)* 397 (1997) 1.
- [3] A.D. Headley, J. Nam, *J. Mol. Struct. (Theochem.)* 589–590 (2002) 423.
- [4] A.J.L. Cooper, J.Z. Ginos, A. Meister, *Chem. Rev.* 83 (1983) 321.
- [5] J. Sherman, D. Luciano, A.J. Vander, *Human Physiology: the Mechanisms of Body Functions*, seventh ed., WCB McGraw-Hill, New York, 1998.
- [6] C.E. Dyllick-Brenzinger, A. Bauder, Hs.H. Günthard, *Chem. Phys.* 23 (1977) 195.
- [7] H. Hollenstein, F. Akermann, Hs.H. Günthard, *Spectrochim. Acta* 34A (1978) 1041.
- [8] M.S. Gordon, D.E. Tallman, *Chem. Phys. Lett.* 17 (1974) 385.
- [9] C. van Alsenoy, L. Schaffer, K. Siam, J.D. Ewbank, *J. Mol. Struct. (Theochem.)* 187 (1989) 271.
- [10] J. Murto, T. Raaska, H. Kunttu, M. Räsänen, *J. Mol. Struct. (Theochem.)* 200 (1989) 93.
- [11] K.E. Norris, J.E. Gready, *J. Mol. Struct. (Theochem.)* 258 (1992) 109.
- [12] P. Tarakeshwar, S. Manogaran, *J. Mol. Struct. (Theochem.)* 430 (1998) 51.
- [13] Z. Zhou, D. Du, A. Fu, *Vib. Spect.* 23 (2000) 181.
- [14] I.D. Reva, S.G. Stephanian, L. Adamowicz, R. Fausto, *J. Phys. Chem. A* 105 (2001) 4773.
- [15] K. Harata, N. Sakabe, J. Tanaka, *Acta Crystallogr.* 33B (1977) 210.
- [16] W.J. Ray, J.E. Katon, D.B. Philips, *J. Mol. Struct. (Theochem.)* 74 (1981) 75.
- [17] X. Yang, Z.H. He, K.T. Leung, submitted for publication.
- [18] S. Haq, J.G. Love, H.E. Sanders, D.A. King, *Surf. Sci.* 325 (1995) 230.
- [19] S. Devadas, R.R. Mallik, R. Coast, P.N. Henrisken, *Surf. Sci.* 326 (1995) 327.
- [20] C. Lee, W. Yang, R.G. Parr, *Phys. Rev. B* 37 (1988) 785.
- [21] A.D. Becke, *J. Chem. Phys.* 98 (1993) 5648.
- [22] P.R. Rablen, J.W. Lockman, W.L. Jorgensen, *J. Phys. Chem. A* 102 (1998) 3782.
- [23] M.J. Frisch et al., *Gaussian 98 (Revision A.5.4)*, Gaussian, Inc., Pittsburgh PA, 1998.
- [24] J. Spanget-Larsen, *Chem. Phys.* 240 (1999) 51.
- [25] H. Yoshida, A. Ehara, H. Matsuura, *Chem. Phys. Lett.* 325 (2000) 477.
- [26] S.F. Boy, F. Bernardi, *Mol. Phys.* 19 (1970) 553.
- [27] P.E. Hintze, S. Aloisio, V. Vaida, *Chem. Phys. Lett.* 343 (2001) 159.